

Article

Not peer-reviewed version

---

# Fast Synthesis of Fine Boron Carbide Powders using Electromagnetic Induction Synthesis Method

---

[Anna V. Gubarevich](#)<sup>\*</sup> and Katsumi Yoshida

Posted Date: 4 December 2023

doi: 10.20944/preprints202312.0119.v1

Keywords: boron carbide; powders; electromagnetic induction; synthesis; oxidation resistance



Preprints.org is a free multidiscipline platform providing preprint service that is dedicated to making early versions of research outputs permanently available and citable. Preprints posted at Preprints.org appear in Web of Science, Crossref, Google Scholar, Scilit, Europe PMC.

Copyright: This is an open access article distributed under the Creative Commons Attribution License which permits unrestricted use, distribution, and reproduction in any medium, provided the original work is properly cited.

Article

# Fast Synthesis of Fine Boron Carbide Powders Using Electromagnetic Induction Synthesis Method

Anna V. Gubarevich <sup>1</sup> and Katsumi Yoshida <sup>1</sup>

<sup>1</sup> Laboratory for Zero-Carbon Energy, Institute of Innovative Research, Tokyo Institute of Technology, 2-12-1, Ookayama, Meguro-Ku, Tokyo 152-8550, Japan; hubarevich.h.aa@m.titech.ac.jp

\* Correspondence: hubarevich.h.aa@m.titech.ac.jp; Tel.: +81-3-5734-2960

**Abstract:** Boron carbide (B<sub>4</sub>C) powders with defined stoichiometry, high crystallinity, minimal impurity content, and a fine particle size are imperative for realizing the exceptional properties of this compound in advanced high-technology applications. Nevertheless, achieving the desired stoichiometry and particle size using traditional synthesis methods, which rely on prolonged, high-temperature processes, can be challenging. The primary objective of this study is to synthesize fine B<sub>4</sub>C powders characterized by high crystallinity and a sub-micron particle size, employing a fast, and energy-efficient method. B<sub>4</sub>C powders are synthesized from elemental boron and carbon in a high-frequency induction heating furnace using the Electromagnetic Induction Synthesis (EMIS) method. The rapid heating rate achieved through contactless heating promotes the ignition and propagation of the exothermic chemical reaction between boron and carbon. Additionally, electromagnetic effects accelerate atomic diffusion, allowing the reaction to be completed in an exceptionally short timeframe. The grain size and crystallinity of B<sub>4</sub>C can be finely tuned by adjusting various process parameters, including the post-ignition holding temperature and the duration of heating. As a result, fine B<sub>4</sub>C powders can be synthesized in under 10 minutes. Moreover, these synthesized B<sub>4</sub>C powders exhibit high resistance to oxidation when exposed to air.

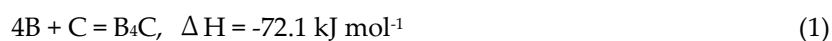
**Keywords:** boron carbide; powders; electromagnetic induction; synthesis; oxidation resistance

## 1. Introduction

Boron carbide (B<sub>4</sub>C) has outstanding properties such as high hardness, low density, high melting point, high temperature stability, good thermoelectric characteristics, and high neutron absorption, making this material attractive for a wide range of applications especially in severe environments, including aerospace, nuclear reactors, and high-temperature thermoelectric conversion [1–3]. B<sub>4</sub>C is commonly used in nuclear applications as a neutron absorber [4]. The most recent applications of B<sub>4</sub>C include boron neutron capture therapy [5], microwave absorbers [6] and photocatalysts [7]. Boron carbide is known to exist as a single phase with carbon concentrations from 8.8 to 20 % [2]. Stoichiometry of boron carbide affects its mechanical, thermoelectric, optical and other properties [1].

B<sub>4</sub>C is commercially produced by carbo-thermic reduction of boric acid or magnesiothermy in the presence of carbon [3]. High temperatures and long time, which are necessary in carbo-thermic reduction or magnesiothermy, result in a large grain size of the product, requiring time- and energy-consuming steps of crushing and grinding to obtain fine powders, necessary, for example, for fabrication of dense ceramics.

High-technology applications of B<sub>4</sub>C require powders with high purity, precise stoichiometry and fine particle size [4–7]. Direct synthesis of B<sub>4</sub>C from boron and carbon (Equation 1) can address issues of purity and stoichiometry.



Boron and carbon are thoroughly mixed and compacted into pellets, which are then heated at temperatures >1500 °C [3]. Although this method is more expensive than carbothermal reduction one,

it is preferable when boron to carbon ratio and high phase purity are important. Still, due to long time treatment at high temperatures the product is coarse and requires crushing, grinding, and ball-milling. While recent reports have introduced innovative synthesis methods for B<sub>4</sub>C particles with varying sizes and morphologies [6], there is no widely accepted approach for producing high-purity, fine B<sub>4</sub>C powders. Moreover, there is an increasing demand to promote environmentally friendly and energy-efficient methods for materials synthesis, propelled by efforts to mitigate the climate crisis.

Combustion synthesis, also known as self-propagating high-temperature synthesis (SHS), is a fast, low energy-consuming and low carbon-emission method for the synthesis of ceramic powders including carbides, nitrides, borides, oxides, and more [8,9]. Combustion synthesis exploits highly exothermic chemical reactions, where the heat generated during the reaction promotes and sustains the reaction itself. In a self-propagating mode, the reaction is initiated by a high-energy pulse, such as brief heating achieved by passing an electric current through a tungsten filament. Once ignited, the reaction propagates without the need for additional external energy input. An important parameter for assessing the feasibility of reaction propagation is the adiabatic temperature, which represents the maximum temperature attainable when all the heat generated during the reaction remains within the system. If the adiabatic temperature falls below a certain threshold, typically around 1800 K, the reaction cannot self-propagate. In such cases, alternative techniques like volume combustion (thermal explosion), chemical ovens, or combustion under elevated temperatures may be employed. The direct reaction between boron and carbon is exothermic (Equation 1), but enthalpy is low (-72.1 kJ mol<sup>-1</sup>) and the adiabatic temperature is only 955 K, therefore combustion synthesis from elements is not self-sustainable [10]; usually highly-exothermic magnesiothermic reaction is used for the combustion synthesis of B<sub>4</sub>C in SHS mode [11]. Evidence of an SHS reaction was observed during the field-activated reactive spark plasma sintering of B<sub>4</sub>C [10,12]. These findings suggest that, with the appropriate field assistance, combustion synthesis of B<sub>4</sub>C is achievable.

Recently, we introduced a novel synthesis technique, which we refer to as electromagnetic induction synthesis (EMIS), for producing various carbide materials [9,15]. EMIS combines combustion synthesis with the assistance of electromagnetic induction. Electromagnetic induction offers rapid, non-contact, and efficient heating of conductive materials, enabling precise power control and adjustable heating rates over a wide range [13,14]. Therefore, combustion synthesis reactions, even with a limited exothermicity, can be initiated and controlled [9]. Additionally, the electromagnetic field directly impacts the sample, accelerating atomic diffusion and enhancing chemical reactions [15]. By integrating combustion synthesis with electromagnetic induction assistance, it is possible to significantly reduce the time, temperature, and energy required for synthesis when compared to traditional synthesis techniques [9,15].

In this study, we demonstrate the efficient synthesis of fine B<sub>4</sub>C powders in a short timeframe using EMIS. The product properties are controlled by optimizing process parameters, including holding temperature and time. Furthermore, we show that the B<sub>4</sub>C powders synthesized through this method have high crystallinity which contributes to the improved resistance to oxidation when subjected to heating in air.

## 2. Materials and Methods

Amorphous boron (0.8 μm, Rare Metallic) and carbon black (80 nm, Asahi Thermal) powders were mixed in stoichiometric proportion with addition of ethanol using a SiC mortar with pestle. Then powders were dried in vacuum drying oven at 70 °C overnight. After drying mixtures were uniaxially pressed into pellets at 10 MPa pressure. A pellet was placed into a graphite crucible and covered with a graphite lid. The crucible was set in high-frequency induction heating (HF IH) apparatus (MU-αIV, SK Medical Electron, Japan) and heated under Ar flow. To measure temperature of the samples, an infrared optical pyrometer (working range 600~3000 °C) was used. Basic experimental set-up is shown in Figure 1 (a). The optical pyrometer was focused on the graphite lid as shown in Figure 1 (a). For recording an exothermic peak of the reaction, the graphite lid was taken off and temperature was measured on the top surface of the samples (Figure 1 (b)). The heating program consisted of three steps: preheating at a slow heating rate (300 °C·min<sup>-1</sup>), ignition at a high

heating rate (1000 °C), and postheating (holding) at constant temperature (1900, 1950 and 1970 °C). Finally, the sample was cooled down naturally under Ar flow. The grey-colored lightly sintered product was obtained. The samples ID with the details of heating conditions are shown in Table 1.

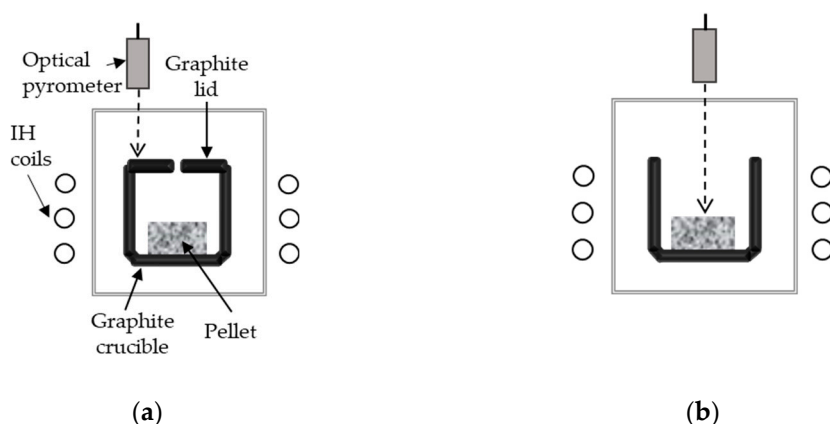


**Figure 1.** EMIS experimental set-up: (a) standard synthesis experiments, (b) recording the exothermic peak.

**Table 1.** Samples synthesized in the present work.

$T_{\max}$ (°C)	Point of T measurement	Holding time at $T_{\max}$ (min)	Sample ID
1700	Sample	0	1
1900		3	2
1900	Graphite lid	5	3
1950		3	4
1970		0	5

Field-emission scanning electron microscopy (FE-SEM, Hitachi S-4800) was applied to characterize microstructure of the fracture surface, grain size and shape of as-synthesized samples. The mean particle size was calculated using ImageJ free software. The samples were lightly ground using a silicon carbide mortar and pestle for further analysis. Crystalline phases were determined using x-ray diffraction method (XRD, Aeris, Panalytical). The specific surface area was analyzed by static manometric nitrogen adsorption at cryogenic temperature (77 K) using a Belsorp 28SA apparatus. The samples were outgassed in vacuum at 300 °C for 2 hours directly prior to measurement. Calculation of the specific surface area (SSA,  $A_{\text{BET}}$ ) was done according to the Brunauer–Emmett–Teller (BET) theory in the range of 0.05–0.3 partial pressure. Average particle size  $d$  (nm) was calculated from  $A_{\text{BET}}$  ( $\text{m}^2 \cdot \text{g}^{-1}$ ) and density of  $\text{B}_4\text{C}$  ( $\rho$ ,  $2.52 \text{ cm}^3 \cdot \text{g}^{-1}$ ) under assumption of spherical particles using Equation 2:

$$d = 6000/A_{\text{BET}} \times \rho \quad (2)$$

Non-isothermal oxidation tests were performed using a thermogravimetry differential thermal analyzer (TG-DTA, Bruker) in ambient air. Synthesized  $\text{B}_4\text{C}$  powders were put into Pt pans and heated in air from room temperature to 700 °C under heating rate of  $10 \text{ }^\circ\text{C} \cdot \text{min}^{-1}$ . Commercial  $\text{B}_4\text{C}$  powder (H.C. Stark, Grade HS,  $0.8 \text{ }\mu\text{m}$  mean particle size) was measured using the same procedure for comparison. An oxidation onset temperature (OOT) was defined as the temperature at which weight of the sample starts to increase.

### 3. Results and Discussion

#### 3.1. Ignition of the Reaction and Temperature-Time Profiles during Synthesis

Figure 2 (a) shows temperature vs time profile measured during heating without the graphite lid as shown in Figure 1 (b). It can be seen from Figure 2 (a) that after 60 s of slow heating the temperature of the pellet was about 600 °C. When the temperature achieved 800 °C, the heating rate was changed from 300 to 1000 °C·min<sup>-1</sup>. Then after 30 s of fast heating a sharp rise in temperature was observed, which started from 1303 °C. The sharp rise in temperature represents the exothermic peak appeared due to the exothermic reaction between boron and carbon leading to formation of B<sub>4</sub>C (Equation 1). The ignition temperature is close to the values observed in reactive spark-plasma sintering of B<sub>4</sub>C [12]. Maximum temperature of the exothermic peak was 1477 °C. It should be mentioned that the values of temperature measured without lid are always lower than measured on the graphite lid under the same IH power. Therefore actual values of the exothermic peak are expected to be higher, when the graphite lid covers the crucible, providing better thermal insulation. Direct visual observation of sample during heating confirmed sudden rise of light emission associated with a volume combustion reaction between boron and carbon. After sample reached temperature of 1700 °C, IH power was stopped and sample was allowed to cool down under Ar flow. It can be seen from the profile that temperature decreased from 1700 to less than 1000 °C in 2 minutes. One example of a typical temperature profile measured on the carbon lid is shown in Figure 2 (a). There is no temperature peak related to the exothermic reaction due to the low exothermic value of the reaction, which was not enough to affect the temperature of the crucible. Figure 2 (b) shows that temperature can be finely controlled during synthesis.

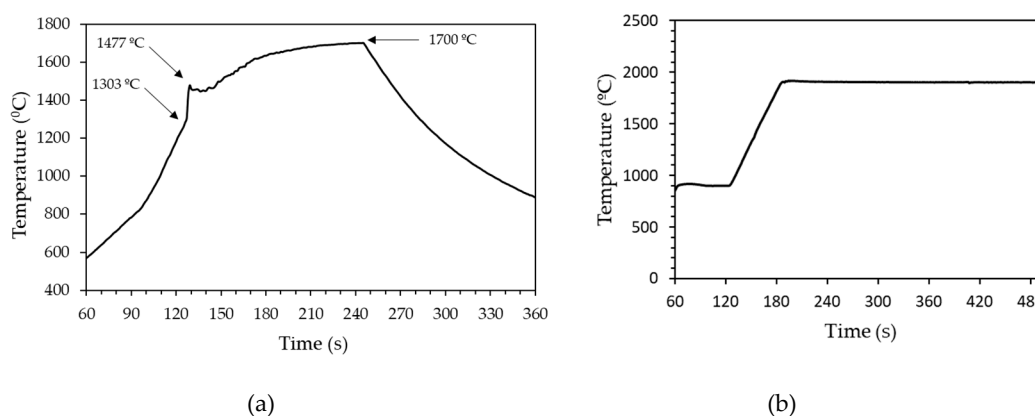


**Figure 2.** Temperature-time profile during synthesis with temperature measured on: (a) the surface of the sample (Sample 1); (b) the graphite lid (Sample 3).

#### 3.2. Characterization of the Synthesized B<sub>4</sub>C

##### 3.2.1. Phase Composition

Figure 3 shows XRD patterns of the synthesized B<sub>4</sub>C samples. All major peaks were attributed to B<sub>4</sub>C. In case of sample 1 peaks of starting materials were observed as well, indicating that the reaction between boron and carbon was not completed at this stage. The exothermicity of the reaction between carbon and boron is not enough to complete the formation of B<sub>4</sub>C, therefore some unreacted elemental carbon and boron remained in the sample. Small peaks of boron trioxide (B<sub>2</sub>O<sub>3</sub>) were identified in sample 1. It is considered that B<sub>2</sub>O<sub>3</sub> was present as an impurity in the starting boron powder. Boiling point of B<sub>2</sub>O<sub>3</sub> is 1860 °C; and sublimation starts at 1500 °C. Sample 1 was heated up to 1700 °C, which is higher than sublimation temperature, but heating time was too short to eliminate all B<sub>2</sub>O<sub>3</sub>. When the additional post-heating step at temperatures higher than boiling point of boron dioxide was applied, the peaks of starting materials and B<sub>2</sub>O<sub>3</sub> became negligible (samples 2-5). Significantly, with the rise in holding temperature from 1900 to 1950 °C, the previously observed

broad halos between 22-24 degrees and 35-38 degrees vanished. This suggests an enhancement in phase purity and crystallinity as the temperature increased.

Heating at the rate as fast as  $1000\text{ }^{\circ}\text{C}\cdot\text{min}^{-1}$  initiates the reaction between carbon and boron due to very high local temperature gradients induced in the sample. Then the reaction between boron and carbon proceeds via mutual diffusion of carbon and boron atoms. However, diffusion of boron and carbon atoms in  $\text{B}_4\text{C}$  is a very slow process due to strong covalent bonds between the atoms and high activation barriers. Moreover, presence of boron dioxide can negatively affect diffusion process. Therefore, in case of sample 1 the reaction between boron and carbon was not completed. When postheating step at  $1900\sim 1970\text{ }^{\circ}\text{C}$  was applied for a short time, the considerable improvement in the phase purity and crystallinity of the samples was observed, indicating acceleration of diffusion under high temperatures. Effective elimination of  $\text{B}_2\text{O}_3$  could promote diffusion and  $\text{B}_4\text{C}$  phase formation. Additionally, in our previous work [16] it was shown, that the induction (eddy) currents induced by high-frequency magnetic field of the coil penetrate through the carbon crucible walls and may affect diffusion processes via electromigration and related phenomena. Therefore, at temperatures beyond  $1900\text{ }^{\circ}\text{C}$  the reaction between boron and carbon was completed in a very short time compared to conventional synthesis [3].

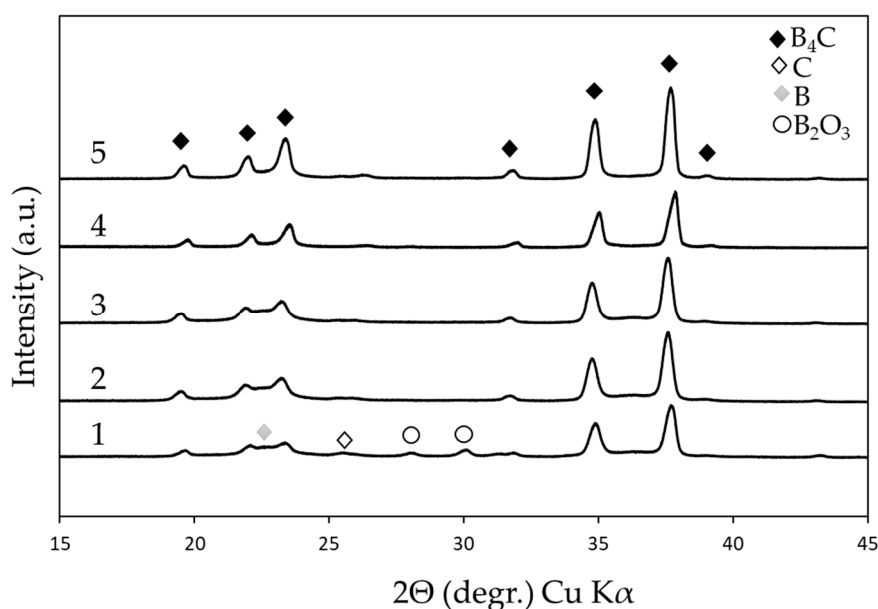


**Figure 3.** XRD patterns of synthesized  $\text{B}_4\text{C}$  powders (sample ID numbers are indicated above the respective lines).

### 3.2.2. Microstructure and Particle Size

Figure 4 shows SEM images of the fracture surface of the synthesized  $\text{B}_4\text{C}$ . It can be confirmed that fine and uniform  $\text{B}_4\text{C}$  grains were synthesized. There was no clear difference in grain shape and size between samples 2 and 3; the grain size is less than  $1\text{ }\mu\text{m}$ . Samples 4 and 5 show larger grain size and better-defined grain shape than samples 2 and 3. Across all samples, the grain shape appeared oval with a low aspect ratio. As depicted in Figure 4 (c, d), heating at  $1950\text{ }^{\circ}\text{C}$  and  $1970\text{ }^{\circ}\text{C}$  (samples 4 and 5) resulted in the partial sintering of grains, a phenomenon not observed in samples 1 and 2. Previous studies have demonstrated that  $\text{B}_4\text{C}$  particles can self-bond without the aid of low-melting additives films [17], and the assistance of IH promotes sintering of  $\text{B}_4\text{C}$  [16]. Samples 4 and 5 exhibited a step-like relief on the surface of  $\text{B}_4\text{C}$  particles, potentially linked to twinning within the grains [18]. In conclusion, it can be inferred that, when the maximum temperature during synthesis is  $1950\text{ }^{\circ}\text{C}$  and higher, the grain size and morphology develop very rapidly, therefore an optimal temperature is not higher than  $1950\text{ }^{\circ}\text{C}$ .

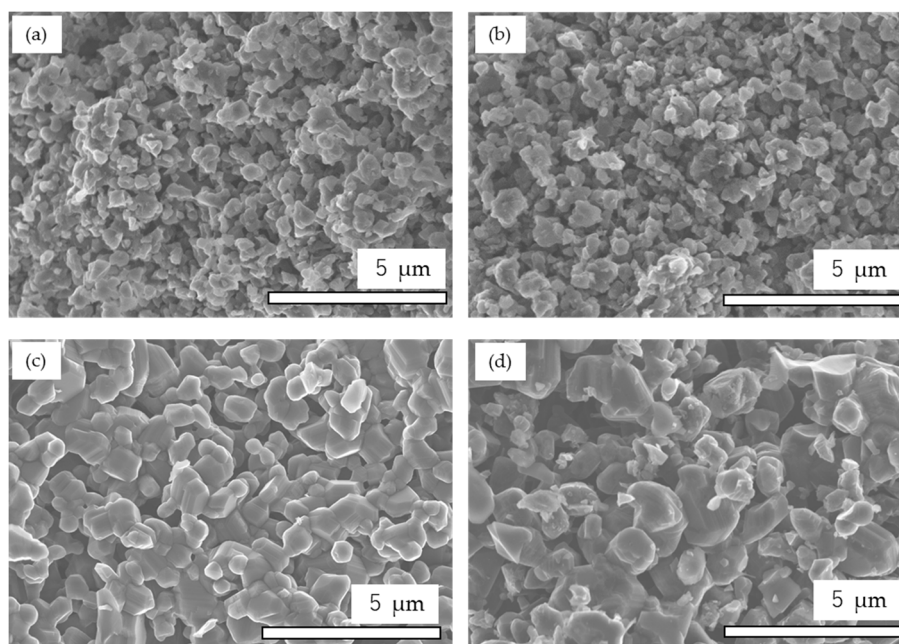


**Figure 4.** SEM images of synthesized B<sub>4</sub>C powders: (a) sample 2; (b) sample 3; (c) sample 4; (d) sample 5.

### 3.2.3. Specific Surface Area

Figure 5 shows adsorption and desorption isotherms of the samples 2 and 5. Other samples produced isotherms of similar shapes. The isotherms shown in Figure 5 belong to the type II of the IUPAC classification [19], thus showing that synthesized powders are non-porous or macroporous materials. Hysteresis between adsorption and desorption isotherms can be related to the presence of macropores. Table 2 shows BET specific surface area (SSA,  $S_{BET}$ ) and average particle size calculated from N<sub>2</sub> gas adsorption data. The SSA of sample 2 is 17.2 m<sup>2</sup>·g<sup>-1</sup> and an average calculated particle size is 138 nm. The calculated particle size is smaller than that observed by SEM (Figure 4 (a) and Table 2). This discrepancy can be related to the non-spherical irregular shape of the particles. Prolongation of heating at 1900 °C from 3 to 5 minutes leads to decrease of the SSA from 17.2 to 11.0 m<sup>2</sup>·g<sup>-1</sup> and increase in the average calculated particle size from 138 to 216 nm. As can be seen from the Table 2, SEM grain size increased much less. When post-heating temperature was increased to 1950 °C, the SSA decreased to 2.3 m<sup>2</sup>·g<sup>-1</sup>, and average particle size increased to 1035 nm. At this temperature the gas-adsorption average particle size and SEM grain size show very close values. Heating to 1970 °C leads to further decrease in the SSA and increase of particle size. As was observed by SEM, heating at 1950 and 1970 °C leads to grain growth and partial sintering of B<sub>4</sub>C, thus decreasing SSA.

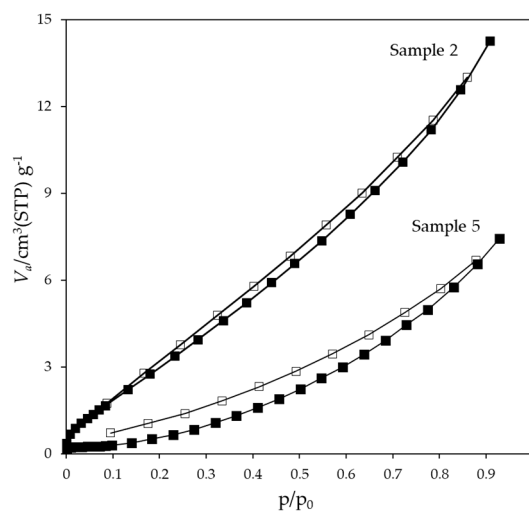


**Figure 5.** Adsorption/ desorption isotherms of the samples 2 and 5.

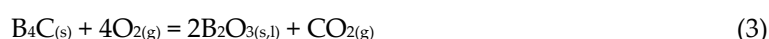
**Table 2.** Specific surface area, grain size and oxidation temperature of the B<sub>4</sub>C powders.

Sample ID	S <sub>BET</sub> (m <sup>2</sup> ·g <sup>-1</sup> )	Average particle size (nm) <sup>1</sup>	SEM grain size (nm) <sup>2</sup>	OOT (°C)
2	17.2	138	450	521
3	11.0	216	480	521
4	2.3	1035	910	584
5	1.5	1550	1060	550

<sup>1</sup> Calculated from N<sub>2</sub> gas adsorption. <sup>2</sup> Calculated from SEM images using ImageJ software.

### 3.3. Non-Isothermal Oxidation of B<sub>4</sub>C Powders

Typical thermogravimetric (TG) curves plotted as weight gain (wt %) versus temperature of the synthesized B<sub>4</sub>C powders and commercial B<sub>4</sub>C powders are shown in Figure 6. The oxidation of B<sub>4</sub>C follows Equation 3 and accompanies a weight gain.



The TG curves clearly indicate that there was no measurable weight gain up to 480 °C. The small weight decrease observed in the commercial powder between 200 and 300 °C is related to the decomposition of boric acid formed on the surface of the powders in air. Beyond 480 °C weight of the commercial B<sub>4</sub>C powder starts to increase rapidly indicating oxidation of B<sub>4</sub>C according to Equation 3. The OOT of the commercial B<sub>4</sub>C powder, determined as the point on the TG curve where weight starts to increase, was 483 °C. The variation of OOT with the synthesized samples is shown in Table 2. The OOT of all synthesized B<sub>4</sub>C powders is higher than that of commercial powder and it increases with increasing post-heating holding temperature from 1900 to 1950 °C. Samples 2 and 3 have very close values of the oxidation temperature, indicating that their stability against oxidation is almost identical. Samples 2 and 3 differ in the postheating time, however, as was shown in the sections 3.2.1 and 3.2.2, their XRD patterns are almost identical and the grain size measured using SEM differs only by 30 nm. Post-heating at 1950 °C leads to improvement of crystallinity (Figure 3) and increases grain size (Figure 4). As a result, OOT of sample 4 is more than 60 °C higher than that of sample 3. OOT of sample 5, which was heated to 1970 °C, is lower than OOT of sample 4. Although both samples, 4 and 5, have similar SEM average grain size (Table 2), the grain size distribution is wider for sample 5, which affects OOT. The particle size has a great influence on oxidation behavior of B<sub>4</sub>C powders [20]. Theoretical calculations showed that powders with 1.52 μm particle size have OOT lower than 500 °C [20]. However, OOT of all samples synthesized in the present work exceeds that value. Therefore, it is concluded that OOT is affected by both the grain size and crystallinity of B<sub>4</sub>C powders.

As can be seen from Figure 6, beyond 600 °C oxidation proceeds very rapidly. The rate of oxidation of the synthesized powders is higher than that of commercial powder. This behavior can be explained by differences in the thickness of B<sub>2</sub>O<sub>3</sub> thin film on the surface of B<sub>4</sub>C particles, which forms when the powders are exposed to air during handling. The thickness of the B<sub>2</sub>O<sub>3</sub> layer influences the time required for oxygen to diffuse through the oxide layer, thus affecting the oxidation rate. The synthesized B<sub>4</sub>C powders were measured soon after the synthesis, therefore B<sub>2</sub>O<sub>3</sub> layer was not formed yet on the surface. As can be seen from the XRD powders, no boron oxide phase was observed for the samples 2-5. The oxidation temperature was found to be independent of the time passed from the synthesis and handling conditions.

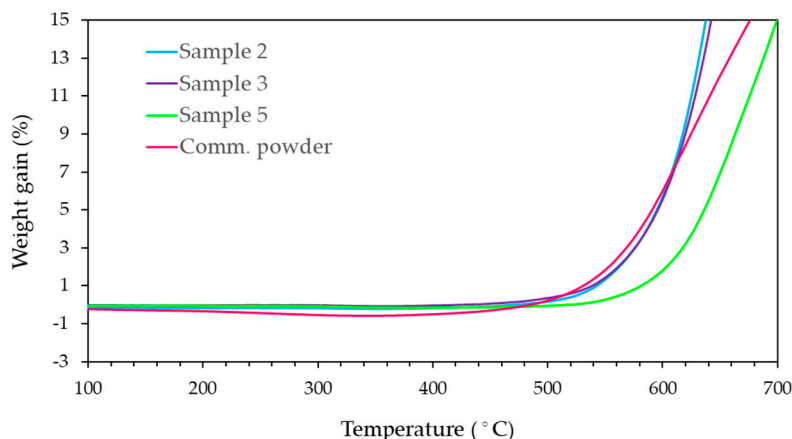


**Figure 6.** TG curves of samples 2, 3, 5, and commercial B<sub>4</sub>C powder.

#### 4. Conclusions

B<sub>4</sub>C powders were successfully synthesized through the high-heating rate, high-temperature, and short-time EMIS method. Phase purity and crystallinity were optimized by varying the conditions of a post-heating step. Powders synthesized with post-heating at 1950 °C for 3 minutes exhibited a graphite-free single-phase composition, a uniform particle size of approximately 1 μm, and a high oxidation onset temperature of 584 °C. This surpasses the oxidation onset temperature of commercial B<sub>4</sub>C powders by more than 100 °C. In summary, the EMIS method proves to be a promising approach for producing phase-pure, fine B<sub>4</sub>C powders, suitable as candidates for advanced technological applications.

**Author Contributions:** Conceptualization, A.G.; methodology, A.G.; validation, A.G., Y.K.; investigation, A.G.; resources, A.G., Y.K.; data curation, A.G.; writing—original draft preparation, A.G.; writing—review and editing, A.G., K.Y.; visualization, A.G.; supervision, A.G., Y.K.; project administration, A.G.; funding acquisition, A.G. All authors have read and agreed to the published version of the manuscript.

**Funding:** This research was supported by JSPS KAKENHI Grant Number 23K04432. 23K04432.

**Institutional Review Board Statement:** Not applicable.

**Informed Consent Statement:** Not applicable.

**Data Availability Statement:** The data presented in this study are available on request from the corresponding author.

**Acknowledgments:** The authors acknowledge Mr. Masamitsu Imai (Tokyo Institute of Technology) for technical support.

**Conflicts of Interest:** The authors declare no conflict of interest. The funders had no role in the design of the study; in the collection, analyses, or interpretation of data; in the writing of the manuscript; or in the decision to publish the results.

#### References

1. Domnich, V.; Reynaud, S.; Haber, R. A.; Chhowalla, M. Boron carbide: structure, properties, and stability under stress. *J. Am. Ceram. Soc.* **2011**, *94*, 3605-3628. doi.org/10.1111/j.1551-2916.2011.04865.x
2. Thevenot, F. Boron carbide - A comprehensive review, *J. Eur. Ceram. Soc.* **1990**, *6*, 205-225. doi.org/10.1016/0955-2219(90)90048-K
3. Suri, A. K.; Subramanian, C.; Sonber, J. K.; Murthy, T. C. Synthesis and consolidation of boron carbide: a review. *Int. Mat. Rev.* **2010**, *55*, 4-40. doi.org/10.1179/095066009X12506721665211
4. Fajar, M.; Gubarevich, A.; Maki, R.S.S.; Uchikoshi, T.; Suzuki, T. S.; Yano, T.; Yoshida, K. Effect of Al<sub>2</sub>O<sub>3</sub> addition on texturing in a rotating strong magnetic field and densification of B<sub>4</sub>C, *Ceram. Int.* **2019**, *45*, 18222-18228. doi.org/10.1016/j.ceramint.2019.06.032

5. Stodolak-Zych, E.; Gubernat, A.; Ścisłowska-Czarnecka, A.; Chadzińska, M.; Zych, Ł.; Zientara, D.; Nocuń, M.; Jeleń, P.; Bućko, M. The influence of surface chemical composition of particles of boron carbide powders on their biological properties, *Appl. Surf. Science* **2022**, *582*, 152380. doi.org/10.1016/j.apsusc.2021.152380
6. Wu, W.W.; Liu, Y.; Zhou, Q.; Liu, L.N.; Chen, X.M.; Liu, P. Microwave absorbing properties of FeB/B<sub>4</sub>C nanowire composite, *Ceram. Int.* **2020**, *46*, 4020-4023. doi.org/10.1016/j.ceramint.2019.10.052
7. Liu, J.; Wen, S.; Hou, Y.; Zuo, F.; Beran, G. J.; Feng, P. Boron carbides as efficient, metal-free, visible-light-responsive photocatalysts. *Ang. Chem. Int. Ed.* **2013**, *52*, 3241-3245. doi.org/10.1002/anie.201209363
8. Patil, K. C.; Aruna, S. T.; Mimani, T. Combustion synthesis: an update. *Curr. opin. solid state mat. sci.*, **2002**, *6*, 507-512. doi.org/10.1016/S1359-0286(02)00123-7.
9. Gubarevich, A. V.; Watanabe, T.; Nishimura, T.; Yoshida, K. Combustion synthesis of single-phase Al<sub>4</sub>SiC<sub>4</sub> powder with assistance of induction heating. *J. Am. Ceram. Soc.* **2020**, *103*, 744-749. doi.org/10.1111/jace.16846
10. Moskovskikh, D.O.; Paramonov, K.A.; Nepapushev, A.A.; Shkodich, N.F.; Mukasyan, A.S. Bulk boron carbide nanostructured ceramics by reactive spark plasma sintering. *Ceram. Int.* **2017**, *43*, 8190-8194. doi.org/10.1016/j.ceramint.2017.03.145.
11. Kovalev, I. D.; Ponomarev, V. I.; Konovalikhin, S. V.; Kovalev, D. Y.; Vershinnikov, V. I. SHS of boron carbide: influence of combustion temperature. *Int. J.SHS*, **2015**, *24*, 33-37. doi.org/10.3103/S1061386215010045
12. Anselmi-Tamburini, U.; Munir, Z. A.; Kodera, Y.; Imai, T.; Ohyanagi, M. Influence of synthesis temperature on the defect structure of boron carbide: experimental and modeling studies. *J. Amer. Ceram. Soc.* **2005**, *88*, 1382-1387. https://doi.org/10.1111/j.1551-2916.2005.00245.x
13. Lucía, O.; Maussion, P.; Dede, E.J., Burdío, J.M. Induction heating technology and its applications: past developments, current technology, and future challenges, *IEEE Trans. Industr. Electr.* **2014**, *61*, 2509-2520. doi: 10.1109/TIE.2013.2281162.
14. Rudnev, V.; Loveless, D.; Cook, R.L. *Handbook of induction heating*, 2nd ed. CRC Press, PA: Taylor & Francis Group, LLC, 2017.
15. Gubarevich, A.V.; Tamura, R.; Yoshida, K. Combustion synthesis of high yield Ti<sub>3</sub>SiC<sub>2</sub> from TiC<sub>0.67</sub> with induction heating assistance, *Ceram. Int.* **2023**, *49*, 23887-23892. doi: 10.1016/j.ceramint.2023.04.236
16. Gubarevich, A.V.; Homma, G.; Yoshida, K. Boron carbide with improved mechanical properties fabricated via rapid pressureless densification with electromagnetic induction assistance. *Scripta Mater.* **2024**, *238*, 115731. doi: 10.1016/j.scriptamat.2023.115731
17. Chen, M. W.; McCauley, J. W.; LaSalva, J. C.; Hemker, K. J. Microstructural characterization of commercial hot-pressed boron carbide ceramics *J. Am. Ceram. Soc.* **2005**, *88*, 1935-1942. doi: 10.1111/j.1551-2916.2005.00346.x
18. Fujita, T.; Guan, P.; Madhav Reddy, K.; Hirata, A.; Guo, J.; Chen, M. Asymmetric twins in rhombohedral boron carbide. *Appl. Phys. Lett.* **2014**, *104*, 021907. doi: 10.1063/1.4861182
19. Thommes, M.; Kaneko, K.; Neimark, A.V.; Olivier, J.P.; Rodriguez-Reinoso, F.; Rouquerol, J. and S., Kenneth, S.W. Physisorption of gases, with special reference to the evaluation of surface area and pore size distribution (IUPAC Technical Report), *Pure Appl. Chem.* **2015**, *87*, 1051-1069. doi: 10.1515/pac-2014-1117
20. Hou, X.; Chou, K. C. Quantitative investigation of oxidation behavior of boron carbide powders in air. *J. Alloys Comp.* **2013**, *573*, 182-186.

**Disclaimer/Publisher's Note:** The statements, opinions and data contained in all publications are solely those of the individual author(s) and contributor(s) and not of MDPI and/or the editor(s). MDPI and/or the editor(s) disclaim responsibility for any injury to people or property resulting from any ideas, methods, instructions or products referred to in the content.